

# Crystallization and preliminary X-ray diffraction analysis of the di-haem cytochrome *c* peroxidase from *Pseudomonas stutzeri*

Cecília Bonifácio, Carlos A. Cunha, Axel Müller, Cristina G. Timóteo, João M. Dias, Isabel Moura and Maria João Romão\*

REQUIMTE, Centro de Química Fina e Biotecnologia, Departamento de Química, Faculdade de Ciências e Tecnologia, Universidade Nova de Lisboa, 2829-516 Monte de Caparica, Portugal

Correspondence e-mail: mromao@dq.fct.unl.pt

Crystals of cytochrome *c* peroxidase from *Pseudomonas stutzeri* were obtained using sodium citrate and PEG 8000 as precipitants. A complete data set was collected to a resolution of 1.6 Å under cryogenic conditions using synchrotron radiation at the ESRF. The crystals belong to space group  $P2_1$ , with unit-cell parameters  $a = 69.29$ ,  $b = 143.31$ ,  $c = 76.83$  Å,  $\beta = 100.78^\circ$ . Four CCP molecules were found in the asymmetric unit, corresponding to a pair of dimers related by local dyads. The crystal packing in the structure shows that the functional dimers can dimerize, as suggested by previous biochemical studies.

Received 9 July 2002

Accepted 13 November 2002

## 1. Introduction

Peroxidases eliminate hydrogen peroxide from cells by catalyzing its reduction to water. Cytochrome *c* peroxidases (CCPs) are haem proteins which contain one or two type *c* haems per monomer. Some well characterized bacterial CCPs are those isolated from *Pseudomonas* (*Ps.*) *aeruginosa* (Ellfolk & Soininen, 1970; Foote *et al.*, 1983), *Paracoccus* (*Pa.*) *denitrificans* (Goodhew *et al.*, 1990), *Nitrosomonas europaea* (Arciero & Hooper, 1994), *Methylococcus capsulatus* (Zahn *et al.*, 1997); *Ps. nautica* (Alves *et al.*, 1999) and *Ps. stutzeri* (Villalaín *et al.*, 1984; Timóteo *et al.*, 2002). Of these, only the CCPs from *Ps. aeruginosa* (Fülöp *et al.*, 1993, 1995) and *N. europaea* (Pappa *et al.*, 1996; Shimizu *et al.*, 2001) have a known crystallographic structure. The *Ps. aeruginosa* CCP crystal structure revealed two histidines coordinating the low-potential haem and one methionine and one histidine coordinating the high-potential haem (Fülöp *et al.*, 1995). In the crystal structure of *N. europaea* CCP, only one histidine coordinates the low-potential haem, leaving one axial coordination position available for binding of hydrogen peroxide (Shimizu *et al.*, 2001). This might account for its activity even in the fully oxidized state, whereas in other CCPs one haem has to be reduced for the enzyme to be fully active.

*Ps. stutzeri* CCP, first identified by Villalaín *et al.* (1984) is a 37 kDa di-haem protein. In *Pa. denitrificans* (Gilmour *et al.*, 1993) and *Ps. stutzeri* (Timóteo *et al.*, 2002) CCP it has been proven that a fully active state of the enzyme is achieved only in the presence of  $\text{Ca}^{2+}$  and it seems that two  $\text{Ca}^{2+}$ -binding sites are present in these enzymes (Gilmour *et al.*, 1995). One of these sites is believed to be that identified in the crystal structures of *Ps. aeruginosa* and *N. europaea*. The other site

has never been observed by crystallography. Spectroscopic changes associated with activation in these CCPs have shown a change of the spin state at the low-potential haem on binding of  $\text{Ca}^{2+}$ . This was interpreted as the loss of coordination of one of the histidines to this haem (Lopes *et al.*, 1998).

Unlike *Pa. denitrificans* CCP, which needs to be reduced with sodium ascorbate for the  $\text{Ca}^{2+}$ -binding site responsible for activation to become fully loaded, *Ps. stutzeri* CCP was isolated with the high-affinity  $\text{Ca}^{2+}$ -binding site fully occupied, in a dimeric form that is active as soon as it becomes reduced by sodium ascorbate. The affinity of this site for  $\text{Ca}^{2+}$  is so high that its dissociation can only be achieved by incubation of the enzyme with EGTA. A low-affinity  $\text{Ca}^{2+}$ -binding site also seems to exist that was empty or only partially occupied in the isolated enzyme (Timóteo *et al.*, 2002). Based on these facts, knowledge of the crystal structure of *Ps. stutzeri* CCP will allow identification of the high-affinity  $\text{Ca}^{2+}$ -binding site and a better understanding of the enzymatic activation mechanism of CCP.

## 2. Material and methods

### 2.1. Protein purification

*Ps. stutzeri* ATCC 11607 cells were grown at 303 K and harvested by centrifugation as described in Timóteo *et al.* (2002). Spheroplasts were prepared according to Goodhew *et al.* (1990). CCP was purified at 277 K: supernatant was loaded onto a DEAE-52 column and concentrated on a small DEAE-52 column and the elutant was then applied onto a Sephadex G 150-50 molecular-exclusion column. The fraction containing CCP was concentrated in a Vivaspin-4 apparatus and the resultant fraction was applied onto a hydroxylapatite column. The purification of CCP, carried out at 277 K,

had to be a rapid operation in order to prevent proteolysis. Peroxidase activity was measured after each purification step according to Gilmour *et al.* (1994). The purity was checked from the absorbance ratio between the bands at 410 and 280 nm as well as by SDS-PAGE. The pure CCP was stored at 203 K in aliquots of 50  $\mu\text{l}$  at 10 mg ml<sup>-1</sup> in 10 mM Tris pH 8.0 (Timóteo *et al.*, 2002).

## 2.2. Crystallization

The initial crystallization screens took place at two different temperatures, 277 and 293 K, using a modified version of the sparse-matrix method of Jancarik & Kim (1991). Crystals appeared at both temperatures within a few days in several conditions containing different salts, buffers and polyethylene glycols (PEG) of different molecular weights. Further experiments were made to try to improve the crystals. Crystals grown in a solution of 20% PEG 8000 and potassium phosphate were optimized by microseeding, but the crystals diffracted poorly and were twinned. The microseeding technique was also used to improve crystals grown in a solution of 12% PEG 3350 and magnesium chloride with MES [2-(*N*-morpholino)ethanesulfonic acid] buffered at pH 6.5, but these crystals were also twinned. In one of the other conditions studied, crystals grew in a solution of 20% PEG 3350, 20% 2-propanol and sodium citrate buffer at pH 5.5; after several experiments, these crystals could be optimized and were not twinned. The best crystals were obtained at 277 K using droplets of 2  $\mu\text{l}$  of protein solution at 10 mg ml<sup>-1</sup> in 10 mM Tris buffer pH 8.0 and 2  $\mu\text{l}$  of reservoir solution containing 18% PEG 8000 and sodium citrate buffer at pH 5.5. Red-orange crystals were obtained overnight and grew to a maximum dimension of 0.2 mm.

## 2.3. Data collection and processing

In order to collect a complete data set and to minimize radiation damage, the *Ps. stutzeri* CCP crystals were cryocooled. A suitable cryoprotectant solution was found by adding 30% glycerol to the harvesting buffer (20% PEG 8000 and sodium citrate pH 5.5). Harvesting buffer was added to the crystallization drop, after which a crystal was transferred to a new drop of harvesting buffer and the cryoprotectant solution was slowly added to this drop. After equilibration, the crystal was transferred to a drop of cryoprotectant. The crystal was mounted on a loop and flash-cooled in a stream of

nitrogen gas at 100 K. Synchrotron data from the native crystal were collected to a resolution of 1.6 Å using an ADSC CCD detector at the European Synchrotron Radiation Facility (ESRF, Grenoble) beamline ID14-2. Data were processed with the programs *DENZO* and *SCALEPACK* (Otwinowski & Minor, 1997). Crystals belong to space group *P2*<sub>1</sub>, with unit-cell parameters  $a = 69.29$ ,  $b = 143.31$ ,  $c = 76.83$  Å,  $\beta = 100.78^\circ$ . For the highest resolution shell (1.66–1.60 Å),  $I/\sigma(I)$  was 3.5 and the completeness was 99.0%, but  $R_{\text{merge}}$  was 41.1%. For this reason, data were only used in the resolution range 30.0–1.66 Å. The data-processing statistics for this resolution range are presented in Table 1.

## 3. Results and discussion

According to Matthews volume calculations (Matthews, 1968), three, four or five molecules (MW = 37 kDa) may be present in the asymmetric unit, corresponding to solvent contents of 63.3, 51.0 and 38.8%, respectively. A self-rotation function was calculated using data in the resolution range 15.0–2.5 Å and a search radius of 20.0 Å, employing the program *MOLREP* (Collaborative Computational Project, Number 4, 1994; Vagin & Teplyakov, 1997). In the self-rotation function for  $\chi = 180^\circ$ , in addition to the peaks originating from the crystallographic axis, six other peaks corresponding to three twofold NCS axes are observed (Fig. 1). No peaks were observed for the search performed for  $\chi = 90^\circ$  and for  $\chi = 120^\circ$ , indicating the absence of fourfold and threefold NCS axes.

The molecular-replacement calculations were performed with the program *MOLREP* (Collaborative Computational Project, Number 4, 1994; Vagin & Teplyakov, 1997) using a maximum resolution of 3.0 Å and the program default values for the minimum resolution and search radius. The sequence of CCP from *Ps. stutzeri* is not yet available, but is expected to be homologous to those from *Ps. aeruginosa* and *Ps. nautica*. The search model used was obtained from the model of CCP from *Ps. aeruginosa* (kindly provided by Vilmos Fülöp; Fülöp *et al.*, 1995), choosing the structurally conserved regions between this model and that of *Ps. nautica* CCP (Dias *et al.*, 2002). The CCP enzymes from these two organisms are 46% identical, with 60%

homology for the amino-acid residues. The model used contained the following residue ranges from the *Ps. aeruginosa* CCP model: 1–17, 20, 25–104, 107–110, 114, 117–141, 146–218, 229–230, 233–240 and 244–322. Both haems were used in the model, but not the calcium ion. Conserved residues in the core of the proteins were kept in the model, while all polar residues at the surface were mutated to alanines.

The cross-rotation function calculation gave four clear peaks above the noise level (Table 2). Since the crystals belong to the polar space group *P2*<sub>1</sub>, in the first translation function each of these cross-rotation peaks gave several solutions with fixed values for the  $x$  and  $z$  coordinates and varying values

**Table 1**

Crystallographic data and data-collection statistics for *Ps. stutzeri* CCP.

Values in parentheses refer to the last resolution shell (1.73–1.66 Å).

X-ray source	ID14-2, ESRF
Wavelength (Å)	0.933
Crystal data	
Space group	<i>P2</i> <sub>1</sub>
Unit-cell parameters (Å, °)	$a = 69.29$ , $b = 143.31$ , $c = 76.63$ , $\beta = 100.78$
Molecules per a.u.	4
Solvent content (%)	51.0
Mosaicity	0.27
Data collection	
Resolution (Å)	30.0–1.66 (1.73–1.66)
Redundancy	3.5 (3.4)
No. of observations	1346465
No. of unique reflections	172125
$R_{\text{merge}}$ (%)	6.3 (28.6)
Completeness (%)	99.4 (99.1)
$I/\sigma(I)$	18.6 (5.1)

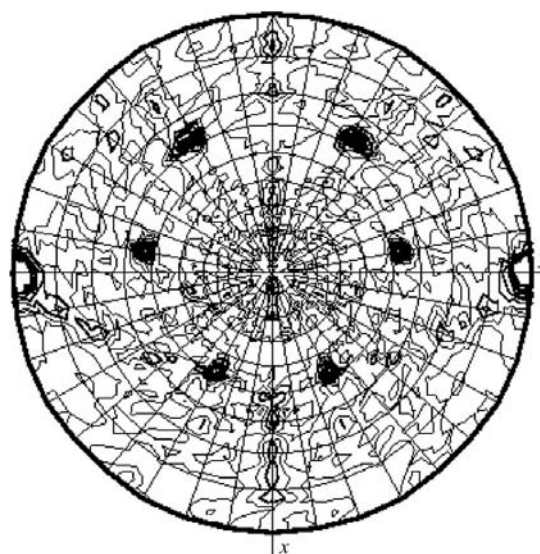


**Figure 1**

Self-rotation function for  $\chi = 180^\circ$  calculated using a resolution range of 15.0–2.5 Å and a search radius of 20.0 Å. The peaks observed correspond to three NCS axes with orientations given by Eulerian angles ( $\alpha$ ,  $\beta$ ,  $\gamma$ ) of (31.81, 54.64, 211.81°), (149.17, 83.44, 329.17°) and (80.17, 72.37, 260.17°). The heights of the peaks are 9.8, 8.7 and  $8.6\sigma$ , respectively.

**Table 2**  
Molecular-replacement data.

(a) Cross-rotation function.  $\alpha$ ,  $\beta$  and  $\gamma$  are Eulerian angles. The peak heights are given in  $\sigma$  units; the highest peak height for the noise was  $5.24\sigma$ .

$\alpha$ ( $^\circ$ )	$\beta$ ( $^\circ$ )	$\gamma$ ( $^\circ$ )	Peak height
104.17	37.62	279.62	10.25
257.32	41.18	137.80	9.72
355.76	85.38	173.50	8.21
7.99	84.42	245.19	8.18

(b) First translation function.  $X_{\text{frac}}$ ,  $Y_{\text{frac}}$  and  $Z_{\text{frac}}$  are fractional Cartesian coordinates; CC is the correlation coefficient.

$X_{\text{frac}}$	$Z_{\text{frac}}$	CC	$R$ factor
0.326	0.221	0.140	0.573
0.077	0.205	0.095	0.583
0.196	0.134	0.147	0.568
0.065	0.235	0.108	0.582

(c) Translation function. Values in parentheses correspond to the highest noise peaks.

$\alpha$ ( $^\circ$ )	$\beta$ ( $^\circ$ )	$\gamma$ ( $^\circ$ )	$X_{\text{frac}}$	$Y_{\text{frac}}$	$Z_{\text{frac}}$	CC	$R$ factor
355.76	85.38	173.50	0.196	0.038	0.134	0.147 (0.067)	0.568 (0.596)
257.32	41.18	137.80	0.496	0.447	0.235	0.175 (0.131)	0.562 (0.574)
104.17	37.62	279.62	0.324	0.249	0.720	0.352 (0.211)	0.500 (0.546)
7.99	84.42	245.19	0.062	0.411	0.233	0.441 (0.299)	0.461 (0.517)

of the  $y$  coordinate. The correlation coefficients for these solutions were clearly above the noise level. After fixing the best solution for the first translation function, clear peaks were obtained for a second, third and fourth translation function. Each translation function was performed keeping fixed the coordinates of the model for the solutions found in the previous translations and using the packing function. All solutions found in the four translation functions corresponded to one of the peaks found in the cross-rotation function. The solution from the fourth rotation function had a correlation coefficient of 0.441 and an  $R$  factor of 0.461 (the correlation coefficient for noise solutions was about 0.3 and an  $R$  factor was about 0.5). The packing of the four translation solutions showed a dimer of dimers in the asymmetric unit that are related by a twofold NCS axis perpendicular to the two

local dyads relating the monomers in the dimers.

Biochemical studies suggest that the active enzyme is a homodimer, as found in other homologous di-haem peroxidases (Gilmour *et al.*, 1994; Alves *et al.*, 1999; Timóteo *et al.*, 2002). A similar dimeric structure has been observed in the crystal structures of homologous enzymes and has been suggested to be the functional entity (Fülöp *et al.*, 1995; Shimizu *et al.*, 2001; Dias *et al.*, 2002). The crystal packing in the structure of CCP from *Ps. stutzeri* also shows this same dimer, although in this case a homotetramer is constituted of a dimer of functional dimers (see crystal packing in Fig. 2). This tetramer constitutes one asymmetric unit and forms a bound entity through the intermolecular contacts within its constituting monomers. This entity may correspond to the four-molecule aggregates that have been observed to occur in solution in previous biochemical studies (Timóteo *et al.*, 2003).

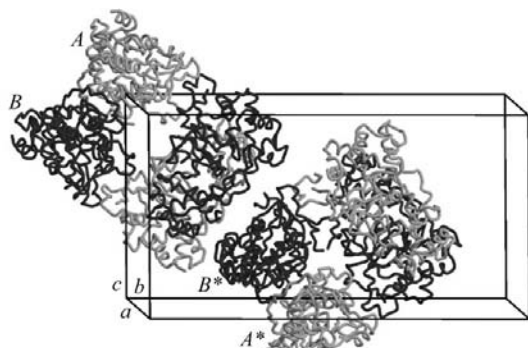


**Figure 2**  
Two homotetramers and one unit-cell box showing the crystal packing.  $A$  and  $B$  form a functional dimer. Figure produced with *MOLSCRIPT* (Kraulis, 1991) and *Raster3D* (Merritt & Bacon, 1997).

This work was supported in part by PRAXIS XXI, PhD grants PRAXIS XXI/BD/13530/97 (JMD), PRAXIS XXI/BD/15752/98 (CAC), PRAXIS XXI/BD/21619/99 (CGT) and project POCTI/QUI/42309/2001. We thank Dr Vilmos Fülöp for providing the CCP *Ps. aeruginosa* coordinates which were used for the molecular replacement. We acknowledge the

EMBL Grenoble Outstation, support for measurements at the ESRF under the European Union TMR/LSF Programme and the beamline scientists Hassan Belrhali and Andy Thompson at beamline ID14-2.

## References

- Alves, T., Besson, S., Duarte, L. C., Pettigrew, G. W., Girio, F. M. F., Devreese, B., Vandenberghe, I., Beuemen, J. V., Fauque, G. & Moura, I. (1999). *Biochim. Biophys. Acta*, **1434**, 248–259.
- Arciero, D. M. & Hooper, A. B. (1994). *J. Biol. Chem.* **269**, 11878–11886.
- Collaborative Computational Project, Number 4 (1994). *Acta Cryst.* **D50**, 760–763.
- Dias, J. M., Bonifácio, C., Alves, T., Moura, J. J. G., Moura, I. & Romão, M. J. (2002). *Acta Cryst.* **D58**, 697–699.
- Ellfolk, N. & Soininen, R. (1970). *Acta Chem. Scand.* **24**, 2126–2136.
- Foot, N., Thompson, A. C., Barber, D. & Greenwood, C. (1983). *Biochem. J.* **209**, 701–707.
- Fülöp, V., Little, R., Thompson, A., Greenwood, C. & Hajdu, J. (1993). *J. Mol. Biol.* **232**, 1208–1210.
- Fülöp, V., Ridout, C. J., Greenwood, C. & Hajdu, J. (1995). *Structure*, **3**, 1225–1233.
- Gilmour, R., Goodhew, C. F., Pettigrew, G. W., Prazeres, S., Moura, I. & Moura, J. J. G. (1993). *Biochem. J.* **294**, 745–752.
- Gilmour, R., Goodhew, C. F., Pettigrew, G. W., Prazeres, S., Moura, I. & Moura, J. J. G. (1994). *Biochem. J.* **300**, 907–914.
- Gilmour, R., Prazeres, S., McGinnity, D. F., Goodhew, C. F., Moura, J. J. G., Moura, I. & Pettigrew, G. W. (1995). *Eur. J. Chem.* **234**, 878–886.
- Goodhew, C. F., Wilson, I. B. H., Hunter, D. J. B. & Pettigrew, G. W. (1990). *Biochem. J.* **271**, 707–712.
- Jancarik, J. & Kim, S.-H. (1991). *J. Appl. Cryst.* **24**, 409–411.
- Kraulis, P. J. (1991). *J. Appl. Cryst.* **24**, 946–950.
- Lopes, H., Pettigrew, G. W., Moura, I. & Moura, J. J. G. (1998). *J. Biol. Inorg. Chem.* **3**, 632–642.
- Matthews, B. W. (1968). *J. Mol. Biol.* **33**, 491–497.
- Merritt, E. A. & Bacon, D. J. (1997). *Methods Enzymol.* **277**, 505–524.
- Otwinowski, Z. & Minor, W. (1997). *Methods Enzymol.* **276**, 307–326.
- Pappa, H., Li, H., Sundaramoorthy, M., Arciero, D., Hooper, A. & Poulos, T. (1996). *J. Struct. Biol.* **116**, 429–431.
- Shimizu, H., Schuller, D. J., Lanzilotta, W. N., Sundaramoorthy, M., Arciero, D. M., Hooper, A. B. & Poulos, T. L. (2001). *Biochemistry*, **40**, 13483–13490.
- Timóteo, G. T., Tavares, P., Goodhew, C. F., Duarte, L. C., Jumel, K., Girio, F. M. F., Harding, S., Pettigrew, G. W. & Moura, I. (2003). In the press.
- Vagin, A. & Teplyakov, A. (1997). *J. Appl. Cryst.* **30**, 1022–1025.
- Villalain, J., Moura, I., Liu, M. C., Payne, W. J., LeGall, J., Xavier, A. V. & Moura, J. J. G. (1984). *Eur. J. Biochem.* **141**, 305–312.
- Zahn, J. A., Arciero, D. M., Hooper, A. B., Coats, J. R. & DiSpirito, A. A. (1997). *Arch. Microbiol.* **168**, 363–372.